Entropy generation in laminar boundary layers of non-ideal fluid flows

Pini, Matteo; De Servi, Carlo

DOI
10.1007/978-3-030-49626-5_8

Publication date
2020

Document Version
Final published version

Published in
Non-Ideal Compressible Fluid Dynamics for Propulsion and Power - Selected Contributions from the 2nd International Seminar on Non-Ideal Compressible Fluid Dynamics for Propulsion and Power, NICFD 2018

Citation (APA)
Pini, M., & De Servi, C. (2020). Entropy generation in laminar boundary layers of non-ideal fluid flows. In F. di Mare, A. Spinelli, & M. Pini (Eds.), *Non-Ideal Compressible Fluid Dynamics for Propulsion and Power - Selected Contributions from the 2nd International Seminar on Non-Ideal Compressible Fluid Dynamics for Propulsion and Power, NICFD 2018* (pp. 104-117). (Lecture Notes in Mechanical Engineering). SpringerOpen. https://doi.org/10.1007/978-3-030-49626-5_8

Entropy Generation in Laminar Boundary Layers of Non-Ideal Fluid Flows

Matteo Pini[1(✉)] and Carlo De Servi[2]

[1] Faculty of Aerospace Engineering, Propulsion and Power, Delft University of Technology, Kluyverweg 1, 2629 HS Delft, The Netherlands
M.Pini@tudelft.nl

[2] Thermal Energy Systems, Flemish Institute for Technical Research (VITO), Boeretang 200, 2400 Mol, Belgium

Abstract. This paper documents a numerical study on entropy generation in zero-pressure gradient, laminar boundary layers of adiabatic non-ideal compressible fluid flows. The entropy generation is expressed in terms of dissipation coefficient C_{d} and its dependency on free-stream Mach number, fluid molecular complexity, and flow non-ideality is investigated systematically by means of a boundary layer code extended to treat fluids modeled with arbitrary equations of state. The results of the study show that the trend of dissipation coefficient follows that of an incompressible flow for complex fluid molecules like siloxanes in all thermodynamic and flow conditions. For simpler fluids like CO_2 the trend becomes inversely proportional to the free-stream Mach number and the C_{d} value can significantly reduce in the non-ideal flow regime, where strong thermo-physical property gradients occur near the wall.

Keywords: Boundary layer · Dissipation coefficient · Non-Ideal Compressible Fluid Dynamics · Organic Rankine cycle · Supercritical carbon-dioxide

1 Introduction

Loss mechanisms in internal flow components such as turbomachines and heat exchangers are intimately related to entropy production due to irreversibility in viscous processes [1]. These are induced by mixing in shear layers as well as viscous dissipation in wall-bounded flows. In turbomachinery, boundary layer loss usually accounts for nearly one-half of the total profile loss of a turbine [1], corresponding to one-sixth of the total turbine loss. Its estimate is, therefore, of particular concern to judge whether a certain design is superior or whether desirable flow features, e.g. flow laminarization or delayed laminar-to-turbulent transition, occur around the blade profile.

The magnitude of viscous dissipation in turbomachines depends on fluid flow characteristics, i.e. Reynolds, Mach numbers and arguably the type of fluid molecule, and it can be predicted using different methods. For instance, viscous

F. di Mare et al. (Eds.): NICFD 2018, LNME, pp. 104–117, 2020.
https://doi.org/10.1007/978-3-030-49626-5_8

dissipation can be well approximated as mass-averaged entropy rise resulting from leading to trailing-edge of blades, and this quantity can be computed by means of high-fidelity numerical calculations or experiments performed on single cascades [2–4]. The drawback of this method is that the physical origin of this loss becomes hard to grasp and systematic studies aimed at revealing physical trends and at developing models for conceptual design can only be carried out at the expense of a significant computational effort. A more convenient way to approach the problem is to resort to the integral form of the kinetic energy boundary-layer equation, whereby the rate of dissipation of mechanical energy in the boundary layer explicitly appears [5]. Such rate, expressed in dimensionless form, is commonly referred to as dissipation coefficient [1]. As opposed to the more familiar skin friction coefficient, the value of dissipation coefficient is relatively insensitive to the state of the boundary layer, i.e. the boundary layer shape factor. Therefore, it is of practical use to gain understanding on the influence of free-stream flow parameters on boundary-layer loss and to provide a quantitative indication of the amount of entropy generated in boundary layers of flows typical of components of propulsion and power systems.

The trend of dissipation coefficient in laminar and turbulent regime has been thoroughly characterized in zero-pressure gradient, accelerating, and decelerating boundary layers of incompressible flows [6]. However, no extensive investigation on the effect of the free-stream Mach number has been reported so far and only qualitative evidences can be found [1]. Furthermore, to the authors' best knowledge, no published data are available with regard to the impact of the fluid molecular structure and of the fluid thermodynamic state on the value of the dissipation coefficient. The latter aspects are especially relevant in turbines and compressors used in power systems based on the concept of organic Rankine cycle (ORC), which operate with non-ideal compressible flows [7,8]. The term Non-Ideal Compressible Fluid Dynamics (NICFD) is utilized to indicate the gas dynamics of such flows. The relative importance of boundary layer loss in these turbomachines is not known yet and thus steps forward in fluid-dynamic performance are arguably possible from an improved physical understanding.

The aim of this paper is, thus, to investigate the effect of flow compressibility, fluid molecular complexity, and flow non-ideality, i.e. departure from perfect gas behaviour [9], on the dissipation coefficient in zero-pressure gradient, adiabatic boundary layers of laminar flow, representative of flow problems occurring in turbomachines. The calculations are carried out using a boundary-layer code extended to the computation of thermo-physical fluid properties with arbitrary equations of state.

The paper structure is as follows. Section 2 describes the background and the scope of work. Section 3 documents the methodology. The findings of the analysis are discussed in Sect. 4.

2 Background and Scope of Work

The non-dimensional form of the boundary-layer kinetic energy equation for planar, compressible flow [5] yields

$$\frac{d\theta^*}{dx} + (3 - M_e^2)\frac{\theta^*}{U_e}\frac{dU_e}{dx} = \frac{2\dot{D}}{\rho_e U_e^3}, \tag{1}$$

where θ^* is the kinetic energy thickness, ρ_e, U_e, M_e are the flow properties at the edge of the boundary layer, while $\dot{D}$ represents the rate of dissipation of mechanical energy in the boundary layer. θ^* can be regarded as the defect of kinetic energy that is extracted from the flow and it is therefore the key quantity to characterize losses in internal flow devices. Equation (1) is applicable to both laminar and (time-mean) turbulent flows. As the boundary layer develops along the wall, the kinetic energy defect is altered by the presence of velocity gradients and by the rate of dissipation of mechanical energy. The latter corresponds to the amount of work done by viscous stresses transferred as heat to the fluid which is given by

$$\dot{D} = \int_0^{y_e} \tau_{xy}\frac{\partial U_x}{\partial y}dy, \tag{2}$$

per unit length along the wall and unit depth. For high-speed flows, the temperature variations within the boundary layer are of the order of M_e^2 [5] as compared to the stagnation temperature of the outer flow. Therefore, a proper averaged temperature value should be introduced to turn $\dot{D}$ into an entropy production term $\dot{S}$ due to irreversibility. Alternatively, $\dot{S}$ can be computed by integrating the local entropy generation along the boundary layer thickness

$$\dot{S} = \int_0^{y_e} \frac{\delta\dot{D}}{T} = \int_0^{y_e} \frac{\tau_{xy}}{T}\frac{\partial U_x}{\partial y}dy. \tag{3}$$

The dissipation coefficient for compressible boundary layers can be defined as

$$C_\mathrm{d} = \frac{T_e\dot{S}}{\rho_e U_e^3}. \tag{4}$$

Equation 4 can be further manipulated to obtain the classical expression of the entropy loss coefficient.

$$C_\mathrm{d} = \frac{T_e\dot{S}}{\rho_e U_e^3} = \frac{D}{2L}\frac{LT_e\dot{S}}{\rho_e U_e D\frac{U_e^2}{2}} = \frac{D}{2L}\zeta. \tag{5}$$

The dissipation coefficient is, thus, equivalent to the local normalized entropy production attained in a channel of aspect ratio D/L, with D the channel width, i.e. the pitch between two adjacent blades, and L a characteristic length where the C_d value can be assumed constant. As such, C_d can be directly used as the

ultimate measure of lost performance due to viscous effects in boundary layers of turbomachines.

From Eqs. (2), (3), (4), it can be inferred that C_d is function of the fluid and flow characteristics, namely the boundary layer state, synthetically characterized through the free-stream flow properties and the Reynolds number based on momentum thickness Re_θ or kinetic energy thickness Re_{θ^*}. In analogy with the findings reported in [1], the boundary layer momentum thickness θ is herein used as characteristic length for the definition of the Reynolds number, while the flow properties are conveniently expressed in terms of the free-stream static pressure and temperature P_e, T_e and of the free-stream Mach number M_e. By introducing the reduced form of the thermodynamic properties, i.e. $P_{r_e} = \frac{P_e}{P_c}, T_{r_e} = \frac{T_e}{T_c}$, with P_c, T_c the fluid critical pressure and temperature, C_d can be finally casted in the following general dimensionless form

$$C_\mathrm{d} = f(Re_\theta, M_e, P_{r_e}, T_{r_e}, \gamma), \tag{6}$$

where γ, that is the specific heat ratio of a fluid in the dilute gas state, is used to denote an arbitrary compound. The reduced state variables P_{r_e}, T_{r_e} here account for non-ideal flow effects in place of the compressibility factor z and the fundamental derivative of gas-dynamics Γ [10].

The objective of the present study is to gain quantitative understanding of the impact of compressibility, fluid molecular structure, and NICFD effects on the trend of dissipation coefficient for laminar flows on flat surfaces. Once C_d is determined for given flow condition, it can be utilized, for instance, in the loss model described in [1], to estimate the boundary-layer losses of a turbine or compressor cascade operating in the non-ideal compressible flow regime.

3 Technical Approach

The value of C_d is retrieved by using the in-house boundary-layer code *BLnI*, which allows to solve the steady-state two-dimensional compressible form of the boundary layer equations for ideal and NICFD flows of arbitrary fluids. The thermo-physical fluid properties are obtained via the *RefProp* library implemented in *FluidProp* [11]. To ease the numerical integration of the boundary layer partial differential equations, these are put in a quasi one-dimensional form by using the Falkner-Skan variable transformation adapted for compressible flows, as proposed by [12]. More in detail, the transformed governing equations are obtained by substituting the Cartesian coordinate y with the similarity variable η, whose definition reads

$$\eta = \sqrt{\frac{U_\mathrm{e}}{\mu_\mathrm{e}\rho_\mathrm{e}x}} \int \rho \, dy, \tag{7}$$

and introducing the dimensionless stream function $f(x, \eta)$.

The use of this transformation allows i) to obtain velocity profiles that are weakly dependent on the free-stream Mach number ii) to limit the increase of

the boundary-layer thickness along the x coordinate, with the result that the mesh domain has not to be adapted during the calculations, and iii) to reduce, or even eliminate for the laminar case, the dependence of the equations solution on x. The resulting momentum and energy equations for a two-dimensional zero-pressure gradient boundary layer read [12]

Momentum :

$$(bf'')' + 0.5ff'' = x\left(f'\frac{\partial f'}{\partial x} - f''\frac{\partial f}{\partial x}\right) \tag{8}$$

Energy :

$$(eg' + df'f'')' + 0.5fg' = x\left(f'\frac{\partial g}{\partial x} - g'\frac{\partial f}{\partial x}\right), \tag{9}$$

where a prime denotes differentiation with respect to η. Note that Eqs. (8) and (9) hold for both laminar and turbulent flows described by the Reynolds-averaged Navier-Stokes equations. For the more general case of turbulent flows, the terms in Eq. (8) and (9) are defined as

$$b = CR\left(1+\nu^+\right), \qquad \nu^+ = \frac{\nu_\mathrm{T}}{\nu}, \qquad CR = \frac{\rho\mu}{\rho_\mathrm{e}\mu_\mathrm{e}}, \tag{10}$$

$$d = \frac{CRU_\mathrm{e}^2}{h_{0,\mathrm{e}}}\left[1 - \frac{1}{\mathrm{Pr}} + \nu^+\left(1 - \frac{1}{\mathrm{Pr}_\mathrm{T}}\right)\right], \qquad e = \frac{CR}{\mathrm{Pr}}\left(1 + \nu^+\frac{\mathrm{Pr}}{\mathrm{Pr}_\mathrm{T}}\right), \tag{11}$$

$$f' = \frac{U_\mathrm{x}}{U_\mathrm{e}}, \quad f'' = \frac{1}{U_\mathrm{e}}\frac{dU_\mathrm{x}}{d\eta}, \quad f = \int f'd\eta, \qquad g = \frac{h_0}{h_{0,\mathrm{e}}}. \tag{12}$$

For laminar flows, the terms on the right-hand side of Eqs. (8) and (9) are equal to zero, because the boundary conditions as well as the equations parameters do not vary with the coordinate x. This does not occur in the turbulent regime, since the dimensionless eddy viscosity ν^+ and, though to a less extent, the turbulent Prandtl number Pr_T vary with Re.

The boundary conditions of Eqs. (8) and (9) for an adiabatic flow can be written in terms of transformed variables as

$$f = 0, \qquad f' = 0, \qquad g' = 0, \qquad \text{at } \eta = 0 \tag{13}$$

$$f' = 1, \qquad g = 1 \qquad \text{at } \eta = \eta_\mathrm{e}. \tag{14}$$

From left to right, the boundary conditions in (13) state that, at the wall, there is no mass transfer, fluid velocity is null, and no heat transfer takes place. At the boundary layer edge, the fluid speed and the total enthalpy becomes, instead, equal to those of the free-stream flow, as indicated by the two relations in (14), respectively.

The system of equations is solved through the Keller-Box method [13]. The differential equations are, first, converted into an equivalent first-order system. The derivative terms are, then, approximated by centered finite differences over

a rectangular and nonuniform grid discretizing in space the $x - \eta$ plane. The resulting algebraic system is solved by the Newton's method. The numerical scheme is unconditionally stable and is second-order accurate. The model is validated by comparing the C_{d} trend for incompressible flows with that given by the analytical function reported in [1].

A database of calculations is constructed by systematic application of the numerical model. The examined test cases are reported in Table 1. The reduced conditions for CO_2, Toluene, and siloxane MM are selected to investigate the impact of near-critical and supercritical flow conditions on the dissipation coefficient. The thermodynamic states corresponding to the reduced conditions for CO_2 and MM are displayed on the contours of compressibility factor in Fig. 1.

Table 1. Test cases examined in this study.

Fluid	M_e	T_{r_e}	P_{r_e}
Helium	0.1	1.05	0.1
	1.0	1.05	0.1
	2.0	1.05	0.1
Air	0.1	1.05	0.1
	1.0	1.05	0.1
	2.0	1.05	0.1
CO_2	0.1	1.05	0.1
	1.0	1.05	0.1 1.0 1.2
	2.0	1.05	0.1
Toluene	0.1	1.05	0.1
	1.0	1.05	0.1 1.0 1.2
	2.0	1.05	0.1
MM	0.1	1.05	0.1
	1.0	1.05	0.1 1.0 1.2
	2.0	1.05	0.1

4 Results for Laminar Flow

4.1 Influence of Flow Compressibility

The influence of M_e on the distribution of the flow quantities inside the boundary layer can be observed in Fig. 2, which reports the results for air at $P_{r_e} = 0.1, T_{r_e} = 1.5$. The charts display the dimensionless velocity and temperature profile as function of the transformed coordinate η, the dissipation coefficient, and the entropy loss coefficient at Mach numbers ranging from incompressible to supersonic flow regime. As anticipated, the solutions of the boundary

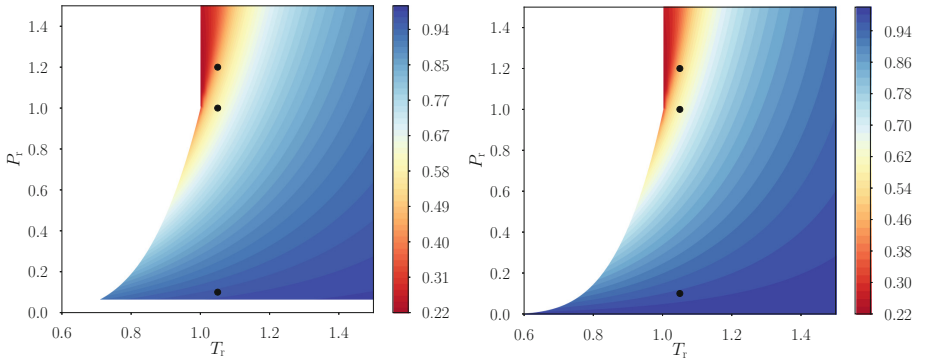

Fig. 1. Contours of compressibility factor z of CO_2 and Siloxane MM. The black dots indicate the reduced conditions of the flow at the edge of the boundary layer considered in the present study.

layer equations are self-similar, i.e. are independent of x. Moreover, the velocity profiles do not vary significantly with the Mach number since the adopted variable transformation removes most of the compressibility effects. The influence of Mach number is, instead, clearly visible in the temperature distribution. The higher the Mach number flow the larger the amount of dissipation $\dot{S}$ and, then, the higher the temperature rise close to the wall. The large dependence of $\dot{S}$ on Mach number becomes apparent by expressing Eq. (3) in terms of the transformed variables

$$\dot{S} = \sqrt{\frac{\rho_\mathrm{e}\mu_\mathrm{e}}{x}} U_\mathrm{e}^{\frac{5}{2}} \int_0^{\eta_\mathrm{e}} \frac{CR}{T} f''^2 d\eta \tag{15}$$

where CR is the Chapman-Rubesin (CR) parameter, whose definition is reported in (10). $\dot{S}$ increases with the 5/2 power of Mach number, if the static thermodynamic conditions of the freestream flow are fixed. The term under the integral sign tends, instead, to decrease as the temperature in the boundary layer increases, but its effect is minor with respect to that of the free-stream velocity. The same considerations can be made based on the Eckert number $Ec = \frac{U_e^2}{c_{p_e} T_e}$, which for a perfect gas simply reads $Ec = M_e^2(\gamma - 1)$. Flows featuring higher values of the Eckert number, namely of Mach number, are subject to stronger thermal gradients within the boundary layer and show an increased amount of dissipation.

Notwithstanding the increase in entropy generation, the dissipation coefficient C_d exhibits the opposite trend and is found to be minimum for the highest Mach number all along the flat plate. Similarly to what done for $\dot{S}$, it is possible to express C_d as

$$C_\mathrm{d} = \frac{1}{\sqrt{Re_\mathrm{x}}} \int_0^{\eta_\mathrm{e}} CR \frac{T_\mathrm{e}}{T} f''^2 d\eta \tag{16}$$

The result points out that the amount of entropy production relative to the kinetic energy of the bulk flow diminishes at increased M_e. At higher Mach number, $\frac{T_e}{T}$ reduces while Re_x increases, and the combination of the two effects leads to a reduction of the dissipation coefficient for high speed flows. At the same time, the reduction of CR close to the wall remains limited in spite of the large temperature gradients at high Mach number.

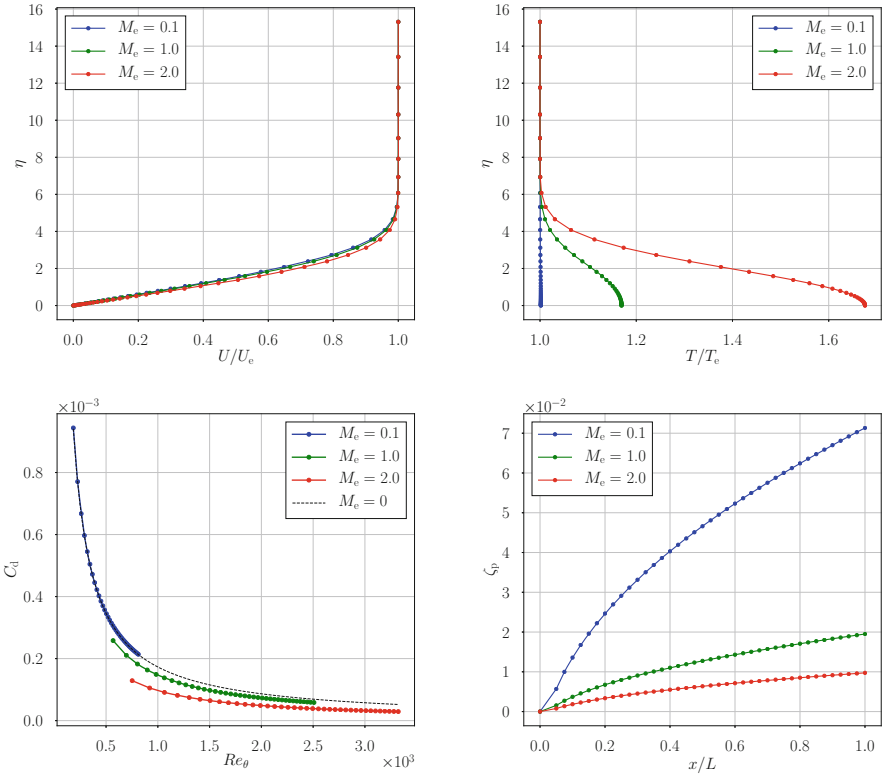

Fig. 2. Dimensionless velocity and temperature profile, dissipation coefficient, and loss coefficient for air at three different Mach numbers. The dashed line in the C_d plot refers to the trend for incompressible flows given in [1].

Similarly to what found for C_d, the profiles losses ζ_p over the plate are lower for high-Mach number flows. ζ_p is shown in the bottom-right chart of Fig. 2 and is computed using the cumulative entropy generated up to a distance x/L from the plate leading edge. The calculated value at $\frac{x}{L} = 1$ would then correspond to the total performance lost caused by viscous effects at the end of the flat plate.

These findings point out that the distribution of C_d is a direct measure of the magnitude of profile losses in turbomachines.

4.2 Influence of Fluid Molecular Complexity

In light of the above considerations, the C_d from one fluid to the other varies according to three parameters: the Eckert number, the Chapman-Rubesin parameter, and Re_x. The results of the analysis made for Helium, CO_2, and Toluene in ideal gas conditions ($P_\mathrm{r} = 0.1, T_\mathrm{r} = 1.05$) at $M_e = 1$ are shown in Fig. 3. The trend of C_d is plotted against Re_θ to facilitate the comparison among the fluids.

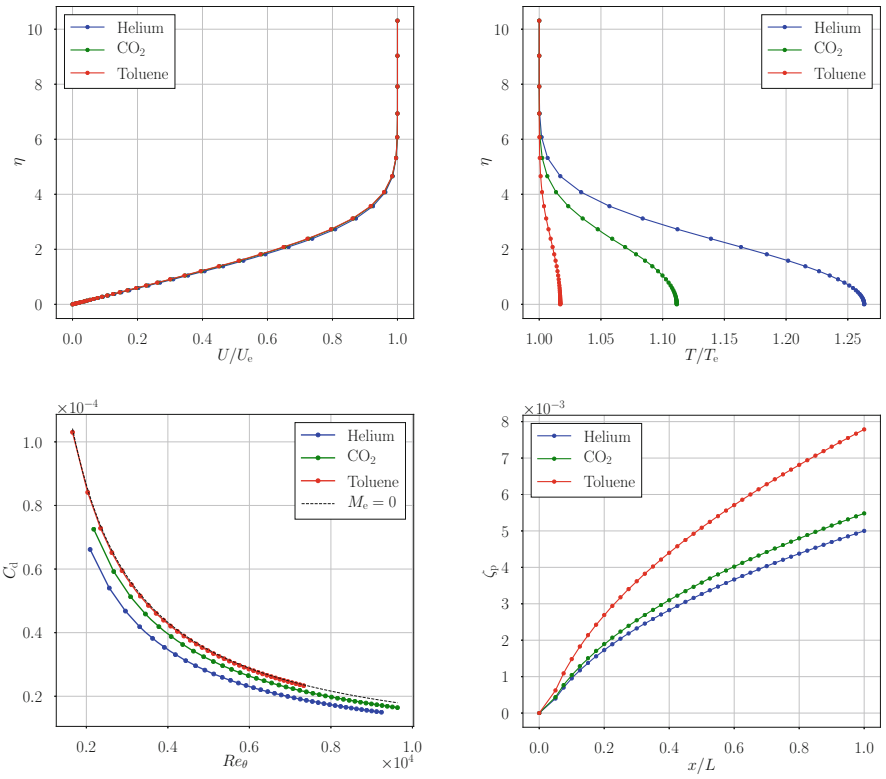

Fig. 3. Dimensionless velocity and temperature profile, dissipation coefficient, and global loss coefficient for Helium, CO_2, and Toluene at $M_e = 1$. The dashed line in the C_d plot refers to the trend for incompressible flows given in [1].

Complex fluids present relatively low values of the Eckert number for M_e characteristic of turbomachinery applications. As a consequence thereof, the boundary layer of highly complex fluids like Toluene and siloxane MM is practically iso-thermal. Similarly, CR does not exhibit appreciable gradients. As a consequence, C_d is only a function of Re_x and its trend resembles that one of an incompressible flow. In fluids made by simple molecules the effect of Ec becomes

significant and may predominate over that of Re_x. This eventually translates into a relevant reduction of C_d. Trends in agreement to those reported in Fig. 3 are also found for $M_e = 2$.

4.3 Influence of NICFD Effects

The impact of NICFD effects on the dissipation coefficient is herein documented. Flat plate simulations at $M_e = 2$ are performed for CO_2 and MM in near-critical and super-critical conditions to better highlight the impact on C_d of variations in the thermo-physical properties. The summary of the performed calculations is reported in Table 2, along with the corresponding Eckert number based on the free-stream quantities.

Table 2. Summary of the simulations performed in the NICFD region.

Fluid	P_{r_e}	T_{r_e}	Ec
CO_2	0.1	1.05	1.03
	1.0	1.05	0.27
	1.2	1.05	0.12
MM	0.1	1.05	0.094
	1.0	1.05	0.033
	1.2	1.05	0.018

It can be observed that the Eckert number undergoes large variations only for CO_2 and that the values for MM are an order of magnitude lower than those of CO_2. The reason thereof is the comparatively higher increase of the specific heat capacity C_p of CO_2 as compared to the other, more complex, fluids when approaching the critical point. These preliminary considerations suggest that the boundary layer of CO_2 in dense gas conditions would behave like the one of an incompressible flow, and thus an increase of C_d as compared to ideal gas conditions should be expected. However, the numerical results for CO_2, displayed in Fig. 4, show the opposite trend. More in particular, though the reduction of Ec for $P_\mathrm{r} = 1.0, 1.2$ entails a decrease of the temperature gradient, i.e. a more uniform temperature profile, within the boundary layer, C_d lowers at fixed Re_θ, in contrast to what found previously. The trend of C_d for MM remains instead essentially insensitive to the fluid thermodynamic state, see Fig. 5.

The different physical behavior between the two fluids can be explained as follows: the velocity profile of CO_2 becomes steeper in dense gas conditions, while it is almost equivalent in all conditions for MM. The change in the velocity distribution of CO_2 can be attributed to the strong reduction of the Chapman-Rubesin parameter close to the wall. Note, however, that reductions of CR also manifest for MM flows in dense gas conditions, but their impact is much more limited on the velocity distribution. In other words, the entropy loss coefficient of

viscous flows in trans- and super-critical state becomes comparatively lower than that of the same fluid stream in ideal conditions provided that strong thermophysical property gradients occur within the boundary layer. Such gradients are characteristic of flows of fluids made by relatively simple molecules like CO_2. On the other hand, NICFD effects are still present in flows of complex fluids like MM and Toluene, but with regard to the trend of C_d they can be considered negligible at flow speed typical of internal flow applications.

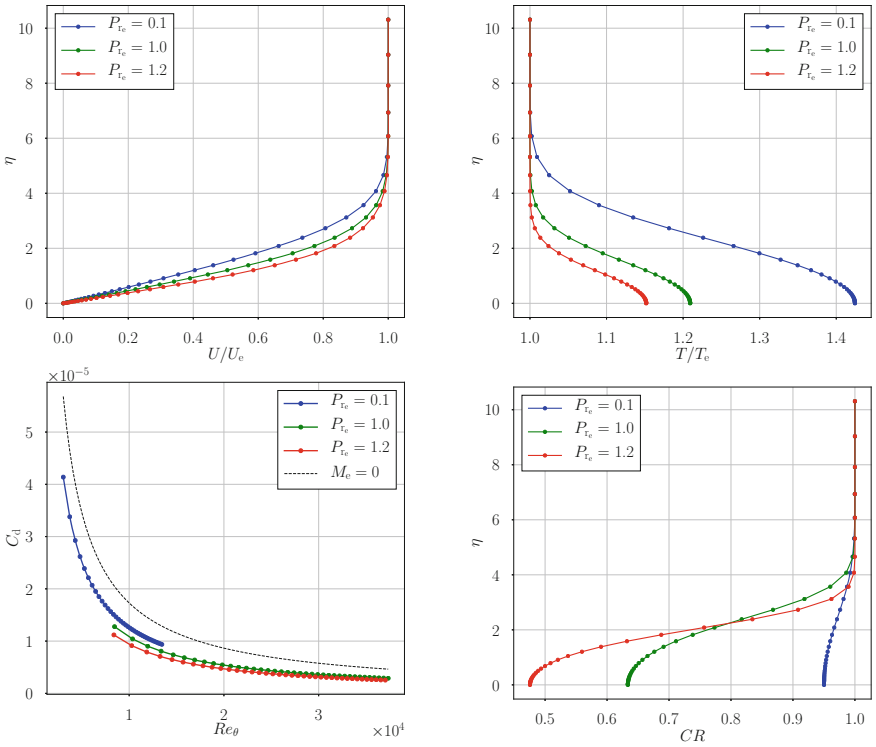

Fig. 4. Results for CO_2 in ideal and NICFD conditions at $M_e = 2$. Top: dimensionless velocity and temperature distribution. Bottom: dissipation coefficient and Chapman-Rubesin parameter within the boundary layer.

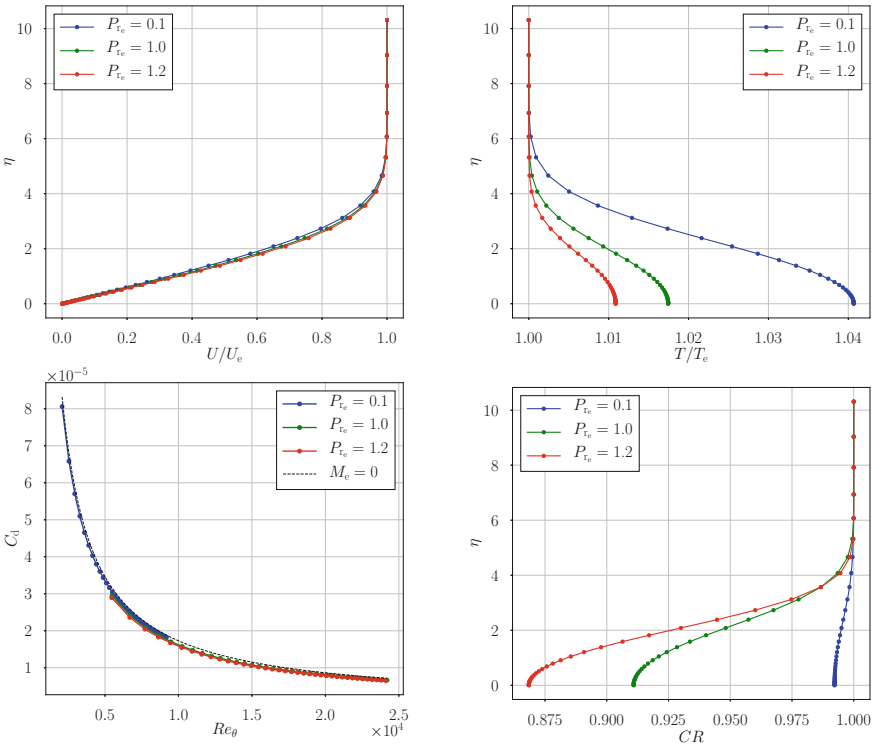

Fig. 5. Results for MM in ideal and NICFD conditions at $M_e = 2$. Top: dimensionless velocity and temperature distribution. Bottom: dissipation coefficient and Chapman-Rubesin parameter within the boundary layer.

5 Conclusions

Viscous dissipation in laminar, compressible boundary layers of ideal and NICFD flows on a flat plate is investigated in this paper. The study is carried out by using a numerical code to solve the two-dimensional compressible boundary layer equations for flows described by arbitrary thermo-physical models. The main findings of the work can be summarized as follows:

1. For a fixed Re_θ, the higher the Mach number the lower the dissipation coefficient C_d. This derives from the simultaneous increase of Re_x and temperature variations $\frac{T}{T_e}$ with increasing Mach number.
2. For a fixed Re_θ, the higher the molecular complexity the higher the dissipation coefficient C_d. Such an increase is principally caused by a progressive reduction of the Eckert number with increasing molecular complexity, which eventually leads to an almost uniform temperature profile inside the boundary layer irrespective of the free-stream Mach number.
3. NICFD effects tend to reduce the value of C_d especially for simple fluid molecules like CO_2. This is attributed to the significant decrease of the

Chapman-Rubesin parameter CR close to the wall due to strong thermophysical property gradients. The reduction of CR at the wall becomes more prominent for increasing Mach numbers.

4. For complex molecules like Toluene and MM the trend of C_{d} can be therefore well approximated by the power law $0.173Re_{\theta}^{-1}$ up to Mach numbers typical of unconventional turbomachinery applications.

Future studies will be devoted to extend the analysis to fully turbulent flows and to investigate the trend of C_{d} for NICFD flows with heat transfer. The ultimate goal is to obtain simplified analytical models for the prediction of C_{d} that can be used for the preliminary design of components of propulsion and power systems operating with non-ideal compressible flows.

Acknowledgements. The authors acknowledge the contribution of D. Dijkshoorn and F. Pizzi to the development and the verification of the boundary layer code.

References

1. Denton, J.D.: Loss mechanisms in turbomachines. In: ASME 1990 International Gas Turbine and Aeroengine Congress and Exposition, p. 40. American Society of Mechanical Engineers, ASME (1993). https://doi.org/10.1115/93-GT-435
2. Mee, D.J.: An examination of the contributions to loss on a transonic turbine blade in cascade. In: ASME 1990 International Gas Turbine and Aeroengine Congress and Exposition, p. 10. American Society of Mechanical Engineers (1990). https://doi.org/10.1115/90-GT-264
3. Michelassi, V., Chen, L.-W., Pichler, R., Sandberg, R.D.: Compressible direct numerical simulation of low-pressure turbines-part II: effect of inflow disturbances. J. Turbomach. **137**(7), 12 (2015). https://doi.org/10.1115/1.4029126
4. Duan, P., Tan, C.S., Scribner, A., Malandra, A.: Loss generation in transonic turbine blading. J. Turbomach. **140**(4), 12 (2018). https://doi.org/10.1115/1.4038689
5. Greitzer, E.M., Tan, C.S., Graf, M.B.: Internal Flow: Concepts and Applications. Cambridge University Press, Cambridge (2007)
6. Schlichting, H., Gersten, K.: Boundary-Layer Theory. Springer, Heidelberg (2016)
7. Harinck, J., Turunen-Saaresti, T., Colonna, P., Rebay, S., van Buijtenen, J.: Computational study of a high-expansion ratio radial organic Rankine cycle turbine stator. J. Eng. Gas Turbines Power **132**(5), 6 (2010). https://doi.org/10.1115/1.3204505
8. Pecnik, R., Rinaldi, E., Colonna, P.: Computational fluid dynamics of a radial compressor operating with supercritical CO_2. J. Eng. Gas Turbines Power **134**(12), 8 (2012). https://doi.org/10.1115/1.4007196
9. Harinck, J., Guardone, A., Colonna, P.: The influence of molecular complexity on expanding flows of ideal and dense gases. Phys. Fluids **21**(8), 086101 (2009). https://doi.org/10.1063/1.3194308
10. Colonna, P., Guardone, A.: Molecular interpretation of nonclassical gas dynamics of dense vapors under the van der Waals model. Phys. Fluids **18**(5), 056101 (2006). https://doi.org/10.1063/1.2196095
11. Colonna, P., der Stelt, T.V., Guardone, A.: FluidProp (version 3.0.6): a program for the estimation of thermo physical properties of fluids. A computer program since 2004 (2018)

12. Cebeci, T.: Convective Heat Transfer. Horizons Pub., Long Beach, California (2002)
13. Cebeci, T., Mosinskis, G., Smith, A.M.O.: Calculation of compressible adiabatic turbulent boundary layers. AIAA J. **8**(11), 1974–1982 (1970). https://doi.org/10.2514/3.6034